Are Multimodal Large Language Models Ready for Omnidirectional Spatial Reasoning?

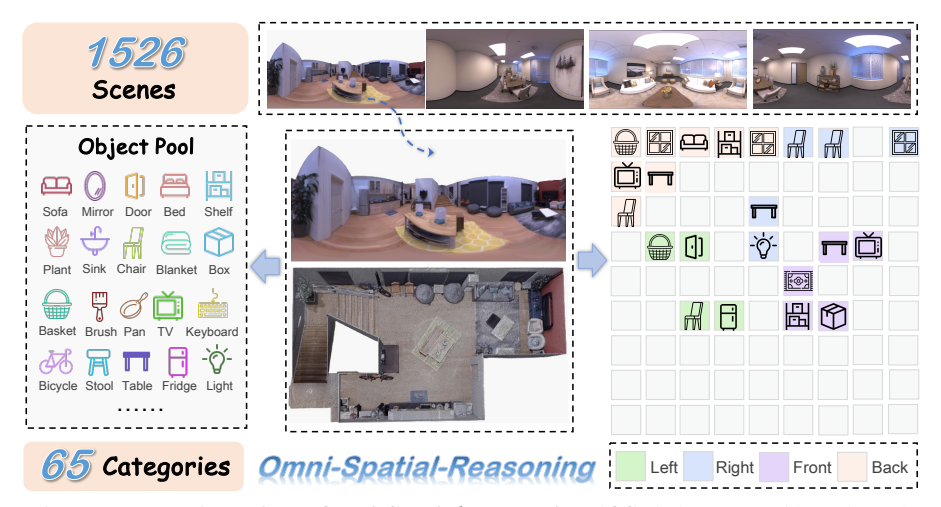


Figure 1: Overview of our *Omni-Spatial-Reasoning (OSR)* dataset and benchmark.

Abstract

The $180^{\circ} \times 360^{\circ}$ omnidirectional field of view captured by 360° cameras facilitates their application across a broad spectrum of downstream tasks such as embodied AI and virtual reality. Despite recent progress in exploring the visual-spatial reasoning capabilities of Multimodal Large Language Models (MLLMs), most existing efforts focus on pinhole-view images, leaving omnidirectional perception underexplored. In this paper, we ask: Are MLLMs ready for omnidirectional spatial reasoning? To address this, we introduce **OSR-Bench**, the first benchmark specifically designed for omnidirectional spatial reasoning. OSR-Bench comprises over 153K diverse Question-Answer (QA) pairs grounded in high-fidelity omnicognitive maps extracted from panoramic indoor scenes, covering key reasoning categories including object counting, relative distance, and relative direction. We further propose a negative sampling strategy that injects non-existent objects into prompts to systematically evaluate hallucination and grounding robustness. To support fine-grained analysis, we design a two-stage evaluation framework that assesses both cognitive map generation and OA accuracy using rotation-invariant matching and both rule-based and LLM-based metrics. We benchmark eight state-of-the-art MLLMs, including GPT-40, Gemini 1.5 Pro, and open-source counterparts, under zero-shot settings. Our results reveal that current models exhibit limited spatial reasoning capabilities under panoramic settings, highlighting the need for more robust and perceptually grounded MLLMs. The established OSR-

^{*}Corresponding author †Equal Contribution

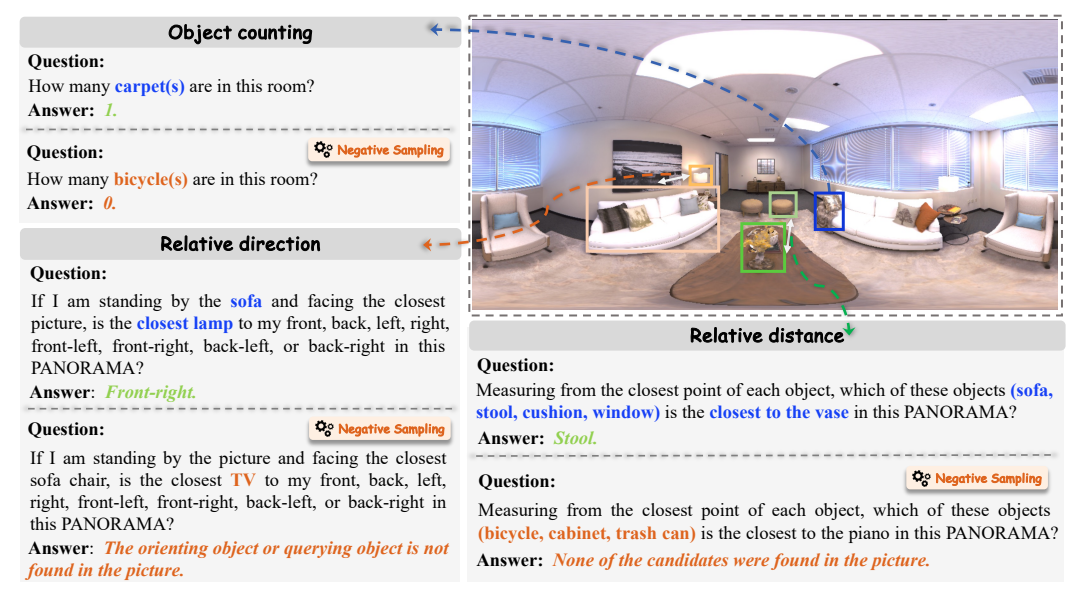


Figure 2: Cases of the established Omni-Spatial-Reasoning dataset.

Bench and source code will be made publicly available at https://huggingface.co/datasets/UUUserna/OSR-Bench.

1 Introduction

Omnidirectional images, captured using 360° cameras, offer a full 180°×360° field of view, enabling comprehensive perception of surrounding environments. This panoramic imaging capability has driven the adoption of omnidirectional sensors in numerous downstream applications, including Augmented Reality (AR), Virtual Reality (VR), and scene understanding tasks [1–6]. Unlike conventional pinhole cameras that provide a limited field of view, 360° cameras capture spatial context in their entirety, making them especially advantageous for embodied AI and spatial reasoning scenarios. Consequently, there has been increasing research interest in leveraging omnidirectional perception for fine-grained scene understanding, particularly in tasks such as semantic segmentation [7–17].

In parallel, the emergence of Large Language Models (LLMs) has brought transformative advances in multi-step reasoning, with growing efforts to extend these capabilities into the visual domain through Multimodal Large Language Models (MLLMs) [18–21]. While MLLMs have demonstrated remarkable performance across modalities such as vision, text, and audio, most existing approaches are built upon 2D planar images from pinhole cameras, thereby under-utilizing the rich spatial information encoded in omnidirectional views. To bridge this gap, we present **OSR-Bench**—the first benchmark specifically designed to evaluate the spatial reasoning abilities of MLLMs in 360° panoramic environments. Built upon the ReplicaPano [22] and DeepPanoContext [23] datasets, OSR-Bench leverages high-fidelity 3D layout annotations to construct ground-truth top-down *omnicognitive maps*, which are used both as evaluation references and as structured priors for generating diverse spatial reasoning questions, as shown in Figure 1.

We develop a scalable, templated QA generation pipeline that produces question-answer pairs covering three key spatial reasoning categories: object counting, relative distance, and relative direction, with cases shown in Figure 2. Each QA pair is derived from the panoramic image and its 3D layout, enabling direct grounding in visual geometry. To assess the robustness of visual understanding, we further introduce a *negative sampling strategy* inspired by recent hallucination detection techniques [24]. By injecting non-existent distractor objects into prompts and QA templates, we generate both matched and mismatched question variants to systematically probe visual grounding fidelity. Our final benchmark comprises over 153,000 QA pairs across 4,100 panoramic images from 1,526 indoor scenes and 65 object categories. OSR-Bench supports fine-grained, interpretable evaluation under both clean and adversarial conditions, offering a rigorous testbed for analyzing the spatial reasoning and robustness of MLLMs in realistic, panoramic settings.

To enable systematic and reproducible evaluation, we design a two-stage assessment protocol tailored for omnidirectional spatial reasoning. The first stage measures a model's ability to construct spatially grounded cognitive maps from panoramic images, whereas the second evaluates its capacity to solve reasoning tasks such as object counting, relative distance, and direction. We adopt Hungarian matching with rotation-invariant F1 scores for cognitive map alignment, and employ both rule-based and LLM-based evaluators to assess question-answering performance, including hallucination sensitivity. We further evaluate a suite of eight state-of-the-art MLLMs spanning both proprietary (e.g., GPT-40, Gemini 1.5 Pro) and open-source families (e.g., InternVL2.5 [25], LLaVA-v1.5 [26], LLaMA3.2-Vision [27], Qwen2.5-VL [28], DeepSeek-VL2 [29], Janus-Pro [30]). All evaluations are conducted in strict zero-shot settings without any task-specific fine-tuning. To ensure methodological consistency and result reproducibility, we apply greedy decoding across all models.

In summary, our work makes the following contributions: (I) We introduce **OSR-Bench**, the first benchmark specifically tailored for evaluating the spatial reasoning abilities of Multimodal Large Language Models (MLLMs) in 360° panoramic environments. (II) We develop a scalable data generation pipeline that constructs over 153,000 high-quality QA pairs across three spatial reasoning categories, grounded in omni-cognitive maps derived from photorealistic indoor layouts. (III) We propose a novel *negative sampling strategy* that injects non-existent distractor objects into both prompts and QA templates, enabling robust evaluation of hallucination and visual grounding fidelity. (IV) We design a two-stage evaluation framework combining rotation-invariant cognitive map matching with both rule-based and LLM-based QA assessment, supporting interpretable and reproducible benchmarking. (V) We conduct a comprehensive evaluation across 8 state-of-the-art MLLMs, both proprietary and open-source, under strict zero-shot settings, establishing the first comparative study of panoramic spatial reasoning in the multimodal era.

2 Related Work and Motivation

Visual Understanding and Reasoning. Visual understanding and reasoning lie at the intersection of computer vision and natural language processing, with tasks like Visual Question Answering (VQA) serving as key benchmarks. Datasets such as VQAv2 [31], GQA [32], and TextVQA [33] have driven progress in this area by testing increasingly complex reasoning skills. More recent benchmarks like SEED-Bench [34], MMBench [35], and MM-Vet [36] extend these efforts to multimodal large language models (MLLMs) across diverse visual-linguistic tasks. For multi-turn dialogue, benchmarks like ConvBench [37] and MMDU [38] further push the field by introducing hierarchical capabilities and multi-image contexts, respectively. However, challenges like object hallucination persist, as highlighted by POPE [24] and NOPE [39], which measure models' tendency to generate false object references. Spatial reasoning has also received attention, with datasets like What's-Up [40] and VSI-Bench [41] evaluating how effectively models handle spatial relationships and cognitive mapping.

Motivation. Despite these advancements, most existing benchmarks focus on standard field-ofview images, limiting their ability to assess spatial understanding in more complex environments. Notably, they overlook the unique challenges of omnidirectional perspectives, which involve handling object relationships, counting, and relative direction in panoramic scenes. To address this gap, we propose OSR-Bench, the first benchmark specifically designed to evaluate spatial reasoning in 360° environments, providing a more comprehensive assessment of MLLMs.

Panoramic Scene Understanding. Panoramic scene understanding presents unique challenges compared to conventional narrow-field vision. The equirectangular projection used for 360° images introduces geometric distortion, while the expanded field of view increases object density and spatial complexity, complicating scene interpretation. Early work [42, 23, 22] in this area focused on specific tasks like room layout reconstruction, recovering instance-level geometry from panoramic images. However, these approaches often produce task-specific outputs (*e.g.*, corner coordinates, mesh vertices) that are not directly compatible with Multimodal Large Language Models (MLLMs). Recent efforts have expanded to fine-grained scene understanding, including semantic segmentation [7–17], aiming to capture richer semantic content. This growth has been accompanied by the creation of specialized panoramic datasets. For example, Pandora [43] focuses on orientation-aware object detection, while 360+x [44] and R3DS [45] provide multimodal annotations for comprehensive scene understanding. Large-scale outdoor datasets like KITTI-360 [46], DensePASS [47], and the Waymo

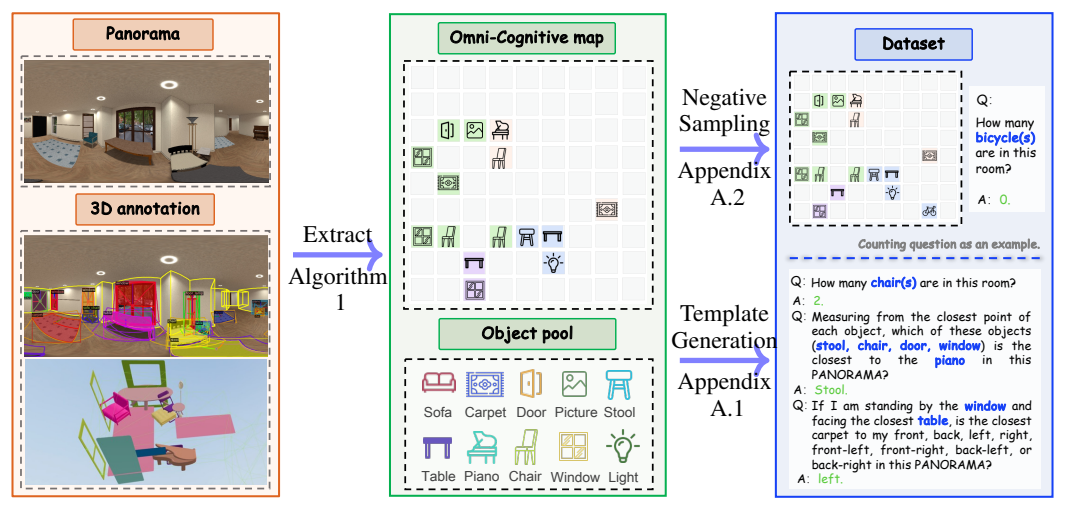


Figure 3: The data generation pipeline of our dataset.

Open Dataset [48] target autonomous driving, while Matterport3D [49] and Stanford2D3D [50] offer richly annotated indoor scans for embodied intelligence.

Motivation. Despite these advancements, existing datasets face several limitations when used to evaluate MLLMs under a unified VQA paradigm: ① *Task mismatch:* Many datasets focus on geometric reconstruction or dense prediction, which are not naturally suited for VQA-style evaluation. ② *Translation overhead:* Converting these tasks into natural language queries requires extensive post-processing, often losing geometric context. ③ *Limited spatial QA coverage:* Current omnidirectional VQA datasets (e.g., Pano-AVQA [51], VQA 360° [52]) lack comprehensive spatial reasoning, particularly for object positions across the full 360° field of view. ④ *Handcrafted bias:* Manually constructed QA pairs may not capture the full complexity of panoramic spatial reasoning, increasing the risk of hallucination. To address these gaps, we propose *OSR-Bench*, a benchmark specifically designed to systematically assess spatial reasoning in panoramic scenes, providing a foundational and open resource for the community.

3 OSR-Dataset & Benchmark

To explore the spatial reasoning ability of existing MLLMs, we develop an omnidirectional question answering construction pipeline to effectively and automatically generate high-quality QA pairs at scale, as illustrated in Fig. 3. The following is the detailed dataset construction pipeline.

3.1 Dataset Construction

Data Collection. Our dataset is primarily built upon two public panoramic scene understanding datasets: ReplicaPano-Dataset [22] and the dataset introduced in DeepPanoContext [23]. Both datasets are derived from iGibson synthetic environments [53], providing photorealistic indoor panoramic scenes with comprehensive layout annotations. These datasets are originally designed for room layout reconstruction tasks. They contain detailed ground truth information about object positions, orientations, and room boundaries, enabling robust omni-cognitive map generation that is critical to our benchmark.

Omni-Cognitive Map Extraction. From the layout annotations in the source datasets, we extract ground truth omni-cognitive maps representing top-down views of each room, as shown in Figure 3. These omni-cognitive maps serve as simplified representations of object locations within the environment, similar to the approach in [41]. These omni-cognitive maps serve two purposes: ① The omni-cognitive maps serve as *ground truth* references for evaluating the spatial understanding capabilities of LLMs that have been prompted to construct cognitive maps prior to addressing spatial reasoning questions, and ② The omni-cognitive maps enable *automatic generation* of diverse spatial reasoning questions with verifiable answers using predefined templates. More specifically, we begin with each panoramic image and its associated 3D layout annotations, from which we extract all

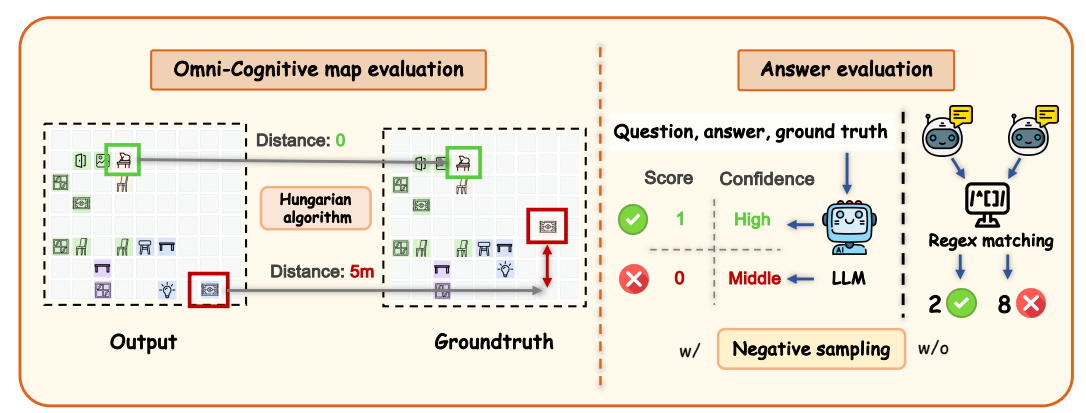


Figure 4: Benchmark Evaluation Pipeline.

Table 1: **Comparison of** *OSR-bench* **with existing QA datasets. Modality**: multimedia input data type; **Auto**: whether the production process is automatic or manual craft **Dis**: presence of negative distractors by negative sampling to test hallucination; **#QAs**: number of QA pairs.

Dataset	Modality	Domain	Auto	Dis	#QAs
Pano-AVQA [51]	360° videos & audio	simple spatial & audio reasoning	×	×	51.7K
VQA 360° [52]	360° images	simple spatial & attributes reasoning	×	×	16K
VIEW-QA [54]	360° videos & audio	daily tasks of the visually impaired	×	×	4K
VSI-Bench [41]	NFOV videos	complex spatial reasoning	\checkmark	×	5K
OSR-Bench(ours)	360° images	complex spatial reasoning	\checkmark	\checkmark	153K

object instances and construct a ground-truth omni-cognitive map representing the top-down layout of that scene. The same extracted objects are simultaneously organized into an object pool. Both the omni-cognitive maps and the object pools are then fed into our QA template generation module, where predefined templates are applied to produce diverse spatial-reasoning questions.

Negative Sampling. Unlike the existing spatial reasoning benchmark VSI-bench [41], which relies solely on ground-truth objects to construct QA templates and generate prompts for cognitive map, our approach addresses an important limitation: *models may prioritize knowledge from textual input while ignoring potential mismatches between visual and textual information*, as well as *hallucination issues in visual information*. Drawing inspiration from POPE [24], we implement negative sampling strategies (Popular Sampling and Adversarial Sampling, see Appendix A.2 for details) by introducing objects that do not exist in each scene. These interference items are incorporated into QA templates and prompt words that guide the model in cognitive map generation, resulting in two versions of our QA dataset. This methodology primarily evaluates a model's visual-spatial understanding capabilities within a single-image panoramic perspective, focusing on three problem categories: object counting, relative distance, and relative direction, as illustrated in Figure 2.

Dataset Overview. Our OSR-Bench comprises 4,100 panoramic images with a total of 65 object categories sourced from 1,526 photorealistic synthetic indoor scenes. For each image, we generate 5 to 10 regular QA pairs for each evaluation category described in the previous paragraph, alongside an equal number of negative sampling QA pairs. To ensure data quality, we implement rigorous controls over the sampling process for both regular and negative sampling QA pairs, thereby eliminating ambiguity and preventing duplication in QA pair generation. In total, our comprehensive benchmark contains approximately 153k QA pairs, which lays a robust foundation for evaluating panoramic spatial reasoning capabilities compared to other existing related benchmarks in Table 1. See Appendix B for more statistical insights.

3.2 Our Evaluation Method

OSR-Bench can be viewed as a two-round visual dialogue task. Accordingly, we adopt a two-stage evaluation framework tailored to omnidirectional spatial reasoning. The first stage measures a model's ability to construct accurate cognitive maps from panoramic images based on a comprehensive prompt. The second stage evaluates the model's capacity to answer specific spatial reasoning questions grounded in the constructed map. The overall evaluation pipeline is illustrated in Figure 4.

Metrics. For cognitive map evaluation, we utilize the Hungarian algorithm to determine the optimal assignment between predicted and ground truth object locations. Given a predicted cognitive map P and a ground truth cognitive map G, where P_i represents the predicted positions of object class i and G_i represents the ground truth positions, we define a distance matrix $D^i \in \mathbb{R}^{|G_i| \times |P_i|}$ where each element D^i_{jk} represents the Euclidean distance between the j-th ground truth position and the k-th predicted position for object class i:

$$D_{jk}^{i} = \sqrt{(G_{j}^{i}[0] - P_{k}^{i}[0])^{2} + (G_{j}^{i}[1] - P_{k}^{i}[1])^{2}}.$$
 (1)

The Hungarian algorithm solves the assignment problem by finding the assignment matrix $X^i \in \{0,1\}^{|G_i| \times |P_i|}$ that minimizes the total distance:

$$\min_{X^i} \sum_{j=1}^{|G_i|} \sum_{k=1}^{|P_i|} D^i_{jk} X^i_{jk},\tag{2}$$

subject to the constraints:

$$\sum_{j=1}^{|G_i|} X_{jk}^i \le 1, \quad \forall k \in \{1, 2, \dots, |P_i|\}, \sum_{k=1}^{|P_i|} X_{jk}^i \le 1, \quad \forall j \in \{1, 2, \dots, |G_i|\}.$$
 (3)

To accommodate potential rotational ambiguities in panoramic perception, we evaluate the cognitive map under rotational transformations and select the one that yields the highest F1 score. For each rotation r, we obtain a transformed prediction P^r and compute:

$$F1^{r} = \frac{2 \times \operatorname{Precision}^{r} \times \operatorname{Recall}^{r}}{\operatorname{Precision}^{r} + \operatorname{Recall}^{r}},$$
(4)

where Precision and Recall are calculated based on matches between P^r and G using a distance threshold of 2.0 grid units. For hallucination assessment, we use CHAIR (Confident Hallucination Assessment in Image Reasoning) metrics such as POPE [24]: CHAIR_S, which indicates whether hallucination occurs in a scene(binary); CHAIR_I, which measures the proportion of hallucinated classes among predicted classes; and CHAIR_instance, which measures the proportion of hallucinated instances among all predicted instances. For regular spatial reasoning problems, we employ regex pattern matching to evaluate model responses against ground truth answers, which typically consist of concise words or phrases. Besides, we adopt category-specific evaluation metrics as follows: ① For *Object counting* tasks, we utilize a percentage-based accuracy measurement—awarding 100% when the model's count exactly matches the ground truth, with scores decreasing proportionally as the numerical difference increases. ② For *Relative distance* and *Relative direction* tasks, we implement binary scoring (correct/incorrect) to assess response accuracy, given the discrete nature of these spatial relationships.

LLM Evaluator For more complex evaluation scenarios, particularly with negative sampling, we adopt an LLM-based evaluator—which has been widely used in the evaluation of open-ended questions [55], due to the challenge of evaluating answers about non-existent objects. The LLM evaluator provides binary scores (0 or 1) and confidence levels (high, medium, low), providing detailed evaluation for ambiguous cases. Compared with traditional rule-based evaluation methods, it demonstrates robustness to linguistic variations in model outputs and maintains evaluation fairness across different models; compared with manual assessment methods, this method is more cost-effective and achieves greater objectivity and reduces bias. The specific prompts used for the LLM evaluator to evaluate each spatial reasoning task are detailed in the Appendix C.3.

3.3 Benchmark Experiments

We comprehensively evaluate eight MLLMs across diverse model families. For proprietary models, we consider Gemini-1.5-Pro [56] and GPT-40 [57]. For open-source models, we evaluate models from InternVL2_5-78B [25], LLaVA-v1.5-13B [26], Llama-3.2-90B-Vision-Instruct [27], Qwen2.5-VL-72B-Instruct [28], deepseek-v12 [29] and Janus-Pro-7B [30]. To ensure methodological rigor and comparative validity, all evaluations are conducted under zero-shot settings without any task-specific fine-tuning. Furthermore, we employ greedy decoding across all models to maximize the reproducibility of our experimental results. See Appendix D for details.

Algorithm 1 Omni-Cognitive Map Extraction

Require: Scene annotations S, Grid size $G = 10 \times 10$

- 1: Extract layout boundaries $(x_{min}, y_{min}, x_{max}, y_{max})$ from S
- 2: Initialize cognitive map C as $G \times G$ grid
- 3: Define mapping function: $(x,y)\mapsto (i,j)$ where $i\leftarrow\lfloor\frac{x-x_{min}}{x_{max}-x_{min}}\cdot G\rfloor, j\leftarrow\lfloor\frac{y-y_{min}}{y_{max}-y_{min}}\cdot G\rfloor$
- 4: **for** each object o with centroid (x, y) in S **do**
- 5: $(i, j) \leftarrow$ mapping of (x, y) to grid coordinates using the defined function
- 6: $C[i][j] \leftarrow C[i][j] \cup o.$ class //Add object class to grid cell
- 7: end for
- 8: $\mathcal{D} \leftarrow$ dictionary where $\mathcal{D}[c]$ is the count of class c in C
- 9: **return** C, \mathcal{D}

Table 3: Comparison of the average scores of the models for each type of question without negative sampling. "w/ cogmap" indicates models were first prompted to generate a cognitive map of the omnidirectional scene prior to answering spatial questions, while "w/o cogmap" indicates models answered questions directly without the cognitive mapping step.

Model	object count		relative distance		relative direction		
	w/ cogmap	w/o cogmap	w/ cogmap	w/o cogmap	w/ cogmap	w/o cogmap	
GPT-4o [57]	0.696	0.645	0.342	0.294	0.216	0.285	
Gemini-1.5-Pro [56]	0.744	0.711	0.417	0.424	0.074	0.109	
Llama-3.2-90B [27]	0.697	0.674	0.368	0.323	0.196	0.123	
Qwen2.5-VL-72B [28]	0.558	0.498	0.299	0.325	0.156	0.181	
InternVL2_5-78B [25]	0.683	0.616	0.365	0.397	0.059	0.087	
LLaVA-v1.5-13B [26]	0.598	0.553	0.245	0.226	0.144	0.169	
deepseek-v12 [29]	0.734	0.579	0.091	0.055	0.129	0.131	
Janus-Pro-7B [30]	0.487	0.405	0.200	0.159	0.068	0.159	

3.3.1 Results

Cognitive Map Generation Capabilities.

As shown in Table 2, proprietary models generally outperform open-source alternatives in generating omni-cognitive maps from panoramic images. Gemini-1.5-Pro achieves the highest F1 score of 0.267, followed by GPT-40 at 0.259. Among open-source models, InternVL2-5-78B forms best with an F1 score of 0.243, approach-

Table 2: **Omni-Cognitive Map Generation Performance.** Model performance on generating omni-cognitive maps from benchmark images with identical prompts, without negative sampling. **Best** results are in bold, and <u>second-best</u> are underlined.

Model	Avg distance \downarrow	Precision	Recall	F1 score
GPT-4o [57]	3.501	0.333	0.219	0.259
Gemini-1.5-Pro [56]	3.475	0.313	0.238	0.267
Llama-3.2-90B-Vision-Instruct [27]	5.991	0.256	0.188	0.212
Qwen2.5-VL-72B-Instruct [28]	4.071	0.307	0.199	0.231
InternVL2_5-78B [25]	5.436	0.291	0.218	0.243
LLaVA-v1.5-13B [26]	8.512	0.184	0.153	0.167
deepseek-v12 [29]	9.607	0.133	0.146	0.124
Janus-Pro-7B [30]	14.467	0.111	0.131	0.120

ing the proprietary models' results. However, there is a substantial gap between model families, with the lowest-performing model (Janus-Pro-7B) scoring only 0.008. Notably, all models exhibit poor performance, with the best precision and recall values reaching only 0.333 and 0.238, respectively, highlighting the challenges in accurately capturing spatial arrangements in omnidirectional contexts.

Impact of Cognitive Maps on Spatial Reasoning. Table 3 reveals interesting patterns regarding the utility of cognitive maps for spatial reasoning tasks. For object counting, all models benefit from having a cognitive map, with improvements ranging from 2% to 15%. However, the impact on relative distance reasoning is mixed: some models (notably GPT-40, Llama-3.2-90B, and deepseek-v12) improve substantially with cognitive maps, while others (Gemini-1.5-Pro, Qwen2.5-VL-72B) perform slightly better without them. Most surprisingly, for relative direction tasks, seven out of eight models perform better without cognitive maps, with only Llama-3.2-90B showing improvement when using cognitive maps. This counterintuitive finding suggests that the imperfect cognitive maps generated by these models may actually interfere with their innate ability to reason about

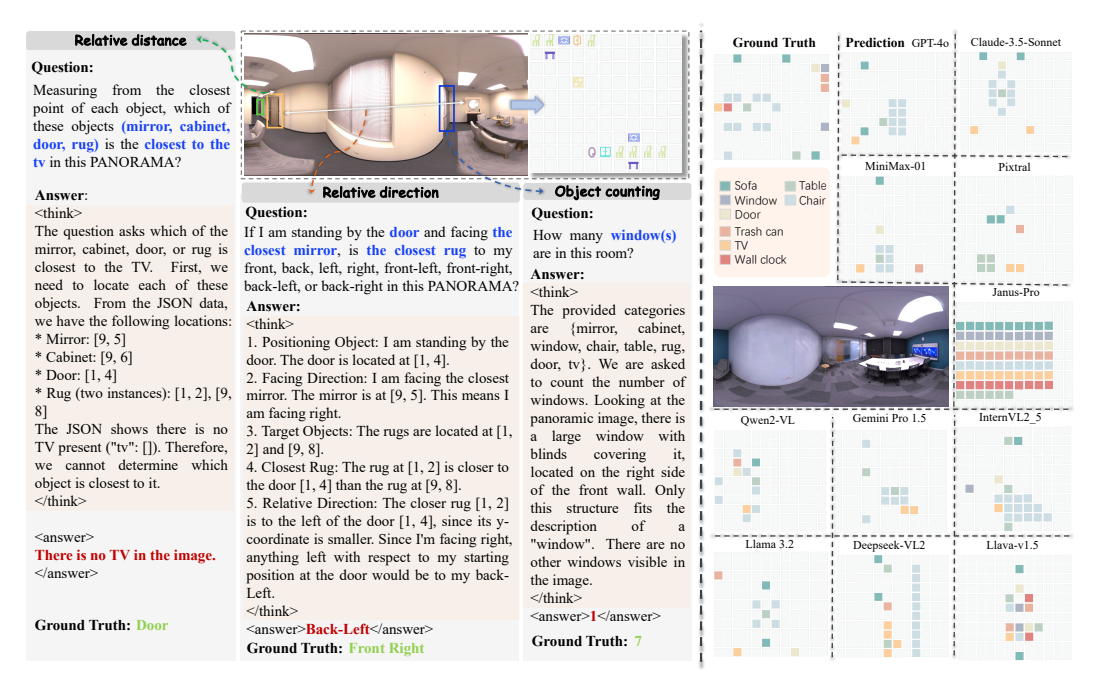


Figure 5: Qualitative examples of omnidirectional spatial reasoning on our OSR-dataset.

Table 4: **Model Performance with Negative Sampling.** Metrics include precision, recall, hallucination scores, and spatial reasoning.

Model	Precision	Recall	CHAIR_S	CHAIR_I	CHAIR_ins	obj count	rel distance	rel direction
GPT-4o [57]	0.303	0.197	0.791	0.198	0.180	0.589	0.435	0.137
Gemini-1.5-Pro [56]	0.269	0.211	0.852	0.202	0.180	0.602	0.441	0.230
Llama-3.2-90B [27]	0.238	0.201	0.875	0.339	0.339	0.535	0.414	0.140
Qwen2.5-VL-72B [28]	0.303	0.189	0.767	0.314	0.306	0.579	0.319	0.232
InternVL2_5-78B [25]	0.278	0.210	0.782	0.248	0.243	0.567	0.378	0.156
LLaVA-v1.5-13B [26]	0.083	0.062	0.884	0.291	0.284	0.523	0.175	0.103
deepseek-vl2 [29]	0.095	0.124	0.844	0.380	0.373	0.641	0.064	0.047
Janus-Pro-7B [30]	0.001	0.002	0.872	0.363	0.277	0.510	0.160	0.004

directional relationships in panoramic images. The cognitive overhead of reconciling potentially inaccurate map representations with the original visual information appears to degrade performance on orientation-sensitive tasks, while still providing benefits for simpler counting operations. The qualitative examples of omnidirectional spatial reasoning are shown in Figure 5 and more case are shown in Appendix E.

Hallucination Robustness. Under the negative sampling condition (Table 4), all models show substantial hallucination tendencies, with CHAIR_S scores ranging from 0.767 to 0.884 (lower is better). Proprietary models are more robust, with GPT-40 achieving the lowest CHAIR_I (0.198) and CHAIR_instance (0.180) scores, indicating fewer hallucinated object classes and instances. Among open-source models, Qwen2.5-VL-72B shows strong resistance, with the lowest CHAIR_S score of 0.767. All models experience performance degradation in spatial reasoning tasks when negative distractor objects are introduced, highlighting limited robustness to interference. Interestingly, hallucination resistance does not perfectly correlate with spatial reasoning performance—deepseek-vl2 achieves the

Table 5: Success rates of different models in constructing properly formatted cognitive maps.

Model	Success Rate (%)
Gemini-1.5-Pro [56]	99.50
GPT-4o [57]	97.50
Qwen2.5-VL-72B [28]	95.60
InternVL2_5-78B [25]	92.40
Llama-3.2-90B [27]	79.15
deepseek-vl2 [29]	44.83
LLaVA-v1.5-13B [26]	10.84
Janus-Pro-7B [30]	4.29

highest object counting score (0.641) despite relatively high hallucination metrics. This discrepancy likely results from deepseek-vl2's architecture, which includes specialized tokens for object localization and reasoning, allowing strong counting capabilities despite weaker hallucination resistance.

Instruction Following and Format Adherence The vast differences in instruction-following capabilities across models are quantitatively demonstrated in Table 5, which shows the success rates in generations.

ating properly formatted cognitive maps. Proprietary models excel at this task, with Gemini-1.5-Pro and GPT-4o achieving success rates of 99.50% and 97.50% respectively. Among open-source models, larger models like Qwen2.5-VL-72B (95.60%) and InternVL2_5-78B (92.40%) approach proprietary-level performance, while smaller models struggle dramatically. The success rate drops to just 10.84% for LLaVA-v1.5-13B and a mere 4.29% for Janus-Pro-7B. This strong correlation between parameter count and instruction following capability explains much of the performance gap observed in Table 2. Models with low success rates in generating properly formatted cognitive maps inevitably achieve poor F1 scores, as their failures stem not just from limitations in visual-spatial understanding but from fundamental difficulties in following structured response protocols for complex spatial representations.

Enhanced Reasoning Through CoT Prompt. The results in Table 6 show that prompting models to use structured reasoning improves performance across most tasks. For example, Gemini-1.5-Pro gains +0.037 in object counting without cognitive maps when guided to think step-by-step (templates in Appendix C.2). This suggests that explicit

Table 6: **Thinking-mode Prompt Result.** Performance improvements for Gemini-1.5-Pro using thinking-mode prompt (with and without Omni-cognitive map) on the non-negatively sampling version of the dataset.

	object count	rel distance	rel direction
w/ omni-cogmap w/o omni-cogmap			

reasoning scaffolds are particularly helpful when models rely solely on internal scene representations. However, gains are generally smaller when cognitive maps are provided, indicating that external spatial representations may overlap with structured reasoning. An exception is relative direction reasoning, which improves significantly (+0.061) with thinking-mode prompts, suggesting that explicit reasoning helps models better integrate directional information from cognitive maps. Overall, structured thinking appears to enhance the effective use of cognitive maps, reducing potential confusion and improving spatial understanding. These findings are further supported by the qualitative results presented in Figure 5.

4 Conclusion

In this paper, we introduced **OSR-Dataset** and **OSR-Bench**, the first benchmarks specifically designed to evaluate the spatial reasoning capabilities of Multimodal Large Language Models (MLLMs) in 360° panoramic environments. Our benchmark includes over 153,000 question-answer pairs across three core spatial reasoning tasks—object counting, relative distance, and relative direction—grounded in high-fidelity 3D scene layouts. To improve evaluation rigor, we proposed a negative sampling strategy to systematically test for hallucination and grounding robustness. We also developed a two-stage evaluation framework that combines rotation-invariant cognitive map alignment with both rule-based and LLM-based question answering, providing fine-grained, interpretable metrics. Our evaluation of eight state-of-the-art MLLMs revealed significant gaps in their spatial reasoning performance under panoramic settings, underscoring the need for more perceptually grounded architectures.

Limitations & Broader Impacts While OSR-Bench provides a comprehensive evaluation framework for omnidirectional spatial reasoning, several limitations remain. The benchmark primarily focuses on indoor environments, which may not fully capture the complexities of outdoor scenes, such as dynamic objects, varying weather conditions, and large-scale spatial structures. Our work advances perceptually grounded MLLMs, with applications in autonomous navigation, augmented reality, and robotics. However, the improved spatial reasoning enabled by this research may raise privacy and surveillance concerns, as panoramic cameras are commonly used in security systems. There is also a risk of misuse in military or surveillance contexts. Researchers should consider these ethical implications when deploying MLLMs trained on spatial reasoning benchmarks.

Maintenance Plan and Future Work To ensure ease of access and future maintenance, the dataset and models evaluated in our paper are hosted on websites and cloud-based storage platforms. And our future work will focus on: (I) Extending to real-world scenes beyond synthetic indoor environments. (II) Evaluating model generalization to out-of-distribution scenarios, including unfamiliar objects and novel scenes. (III) Developing more sophisticated reasoning tasks that capture dynamic scene understanding. (IV) Exploring post-training strategies to enhance panoramic spatial reasoning abilities. OSR-Bench provides a foundation for advancing omnidirectional perception research, and we are committed to expanding this resource for the community.

References

- [1] Lutao Jiang, Jiantao Lin, Kanghao Chen, Wenhang Ge, Xin Yang, Yifan Jiang, Yuanhuiyi Lyu, Xu Zheng, and Yingcong Chen. Dimer: Disentangled mesh reconstruction model. *arXiv preprint arXiv:2504.17670*, 2025.
- [2] Chenfei Liao, Kaiyu Lei, Xu Zheng, Junha Moon, Zhixiong Wang, Yixuan Wang, Danda Pani Paudel, Luc Van Gool, and Xuming Hu. Benchmarking multi-modal semantic segmentation under sensor failures: Missing and noisy modality robustness. *arXiv preprint arXiv:2503.18445*, 2025.
- [3] Xu Zheng, Ziqiao Weng, Yuanhuiyi Lyu, Lutao Jiang, Haiwei Xue, Bin Ren, Danda Paudel, Nicu Sebe, Luc Van Gool, and Xuming Hu. Retrieval augmented generation and understanding in vision: A survey and new outlook. *arXiv preprint arXiv:2503.18016*, 2025.
- [4] Lik-Hang Lee, Tristan Braud, Peng Yuan Zhou, Lin Wang, Dianlei Xu, Zijun Lin, Abhishek Kumar, Carlos Bermejo, Pan Hui, et al. All one needs to know about metaverse: A complete survey on technological singularity, virtual ecosystem, and research agenda. *Foundations and Trends® in Human-Computer Interaction*, 2024.
- [5] Yuanhuiyi Lyu, Xu Zheng, Lutao Jiang, Yibo Yan, Xin Zou, Huiyu Zhou, Linfeng Zhang, and Xuming Hu. Realrag: Retrieval-augmented realistic image generation via self-reflective contrastive learning. arXiv preprint arXiv:2502.00848, 2025.
- [6] Xu Zheng, Yunhao Luo, Pengyuan Zhou, and Lin Wang. Distilling efficient vision transformers from cnns for semantic segmentation. *Pattern Recognition*, 158:111029, 2025.
- [7] Junwei Zheng, Ruiping Liu, Yufan Chen, Kunyu Peng, Chengzhi Wu, Kailun Yang, Jiaming Zhang, and Rainer Stiefelhagen. Open panoramic segmentation. In *ECCV*, 2024.
- [8] Jiaming Zhang, Kailun Yang, Hao Shi, Simon Rei
 ß, Kunyu Peng, Chaoxiang Ma, Haodong Fu, Philip HS Torr, Kaiwei Wang, and Rainer Stiefelhagen. Behind every domain there is a shift: Adapting distortion-aware vision transformers for panoramic semantic segmentation. IEEE Transactions on Pattern Analysis and Machine Intelligence, 2024.
- [9] Jiaming Zhang, Kailun Yang, Chaoxiang Ma, Simon Reiß, Kunyu Peng, and Rainer Stiefelhagen. Bending reality: Distortion-aware transformers for adapting to panoramic semantic segmentation. In CVPR, 2022.
- [10] Xu Zheng, Jinjing Zhu, Yexin Liu, Zidong Cao, Chong Fu, and Lin Wang. Both style and distortion matter: Dual-path unsupervised domain adaptation for panoramic semantic segmentation. In CVPR, 2023.
- [11] Xu Zheng, Tianbo Pan, Yunhao Luo, and Lin Wang. Look at the neighbor: Distortion-aware unsupervised domain adaptation for panoramic semantic segmentation. In *ICCV*, 2023.
- [12] Xu Zheng, Pengyuan Zhou, Athanasios V Vasilakos, and Lin Wang. Semantics distortion and style matter: Towards source-free UDA for panoramic segmentation. In *CVPR*, 2024.
- [13] Xu Zheng, Peng Yuan Zhou, Athanasios V Vasilakos, and Lin Wang. 360SFUDA++: Towards source-free UDA for panoramic segmentation by learning reliable category prototypes. *IEEE Transactions on Pattern Analysis and Machine Intelligence*, 2025.
- [14] Weiming Zhang, Yexin Liu, Xu Zheng, and Lin Wang. GoodSAM: Bridging domain and capacity gaps via segment anything model for distortion-aware panoramic segmentation. In *CVPR*, 2024.
- [15] Weiming Zhang, Yexin Liu, Xu Zheng, and Lin Wang. GoodSAM++: Bridging domain and capacity gaps via segment anything model for panoramic semantic segmentation. arXiv preprint arXiv:2408.09115, 2024.
- [16] Zeyu Cai, Zhelong Huang, Xu Zheng, Yexin Liu, Chao Liu, Zeyu Wang, and Lin Wang. Interact360: Interactive identity-driven text to 360° panorama generation. In *CAI*, 2024.
- [17] Ding Zhong, Xu Zheng, Chenfei Liao, Yuanhuiyi Lyu, Jialei Chen, Shengyang Wu, Linfeng Zhang, and Xuming Hu. OmniSAM: Omnidirectional segment anything model for UDA in panoramic semantic segmentation. *arXiv* preprint arXiv:2503.07098, 2025.
- [18] Yibo Yan, Jiamin Su, Jianxiang He, Fangteng Fu, Xu Zheng, Yuanhuiyi Lyu, Kun Wang, Shen Wang, Qingsong Wen, and Xuming Hu. A survey of mathematical reasoning in the era of multimodal large language model: Benchmark, method & challenges. arXiv preprint arXiv:2412.11936, 2024.

- [19] Jiahao Huo, Yibo Yan, Xu Zheng, Yuanhuiyi Lyu, Xin Zou, Zhihua Wei, and Xuming Hu. MMUnlearner: Reformulating multimodal machine unlearning in the era of multimodal large language models. *arXiv* preprint arXiv:2502.11051, 2025.
- [20] Yiqi Wang, Wentao Chen, Xiaotian Han, Xudong Lin, Haiteng Zhao, Yongfei Liu, Bohan Zhai, Jianbo Yuan, Quanzeng You, and Hongxia Yang. Exploring the reasoning abilities of multimodal large language models (MLLMs): A comprehensive survey on emerging trends in multimodal reasoning. arXiv preprint arXiv:2401.06805, 2024.
- [21] Xiaoqi Li, Mingxu Zhang, Yiran Geng, Haoran Geng, Yuxing Long, Yan Shen, Renrui Zhang, Jiaming Liu, and Hao Dong. ManipLLM: Embodied multimodal large language model for object-centric robotic manipulation. In CVPR, 2024.
- [22] Yuan Dong, Chuan Fang, Liefeng Bo, Zilong Dong, and Ping Tan. PanoContext-Former: Panoramic total scene understanding with a transformer. In *CVPR*, 2024.
- [23] Cheng Zhang, Zhaopeng Cui, Cai Chen, Shuaicheng Liu, Bing Zeng, Hujun Bao, and Yinda Zhang. DeepPanoContext: Panoramic 3D scene understanding with holistic scene context graph and relation-based optimization. In ICCV, 2021.
- [24] Yifan Li, Yifan Du, Kun Zhou, Jinpeng Wang, Wayne Xin Zhao, and Ji-Rong Wen. Evaluating object hallucination in large vision-language models. In EMNLP, 2023.
- [25] Zhe Chen, Weiyun Wang, Yue Cao, Yangzhou Liu, Zhangwei Gao, Erfei Cui, Jinguo Zhu, Shenglong Ye, Hao Tian, Zhaoyang Liu, Lixin Gu, Xuehui Wang, Qingyun Li, Yimin Ren, Zixuan Chen, Jiapeng Luo, Jiahao Wang, Tan Jiang, Bo Wang, Conghui He, Botian Shi, Xingcheng Zhang, Han Lv, Yi Wang, Wenqi Shao, Pei Chu, Zhongying Tu, Tong He, Zhiyong Wu, Huipeng Deng, Jiaye Ge, Kai Chen, Min Dou, Lewei Lu, Xizhou Zhu, Tong Lu, Dahua Lin, Yu Qiao, Jifeng Dai, and Wenhai Wang. Expanding performance boundaries of open-source multimodal models with model, data, and test-time scaling. arXiv preprint arXiv:2412.05271, 2024.
- [26] Haotian Liu, Chunyuan Li, Yuheng Li, and Yong Jae Lee. Improved baselines with visual instruction tuning. In CVPR, 2024.
- [27] Abhimanyu Dubey, Abhinav Jauhri, Abhinav Pandey, Abhishek Kadian, Ahmad Al-Dahle, Aiesha Letman, Akhil Mathur, Alan Schelten, Amy Yang, Angela Fan, Anirudh Goyal, Anthony Hartshorn, Aobo Yang, Archi Mitra, Archie Sravankumar, Artem Korenev, Arthur Hinsvark, Arun Rao, Aston Zhang, Aurélien Rodriguez, Austen Gregerson, Ava Spataru, Baptiste Rozière, Bethany Biron, Binh Tang, Bobbie Chern, Charlotte Caucheteux, Chaya Nayak, Chloe Bi, Chris Marra, Chris McConnell, Christian Keller, Christophe Touret, Chunyang Wu, Corinne Wong, Cristian Canton Ferrer, Cyrus Nikolaidis, Damien Allonsius, Daniel Song, Danielle Pintz, Danny Livshits, David Esiobu, Dhruv Choudhary, Dhruv Mahajan, Diego Garcia-Olano, Diego Perino, Dieuwke Hupkes, Egor Lakomkin, Ehab AlBadawy, Elina Lobanova, Emily Dinan, Eric Michael Smith, Filip Radenovic, Frank Zhang, Gabriel Synnaeve, Gabrielle Lee, Georgia Lewis Anderson, Graeme Nail, Grégoire Mialon, Guan Pang, Guillem Cucurell, Hailey Nguyen, Hannah Korevaar, Hu Xu, Hugo Touvron, Iliyan Zarov, Imanol Arrieta Ibarra, Isabel M. Kloumann, Ishan Misra, Ivan Evtimov, Jade Copet, Jaewon Lee, Jan Geffert, Jana Vranes, Jason Park, Jay Mahadeokar, Jeet Shah, Jelmer van der Linde, Jennifer Billock, Jenny Hong, Jenya Lee, Jeremy Fu, Jianfeng Chi, Jianyu Huang, Jiawen Liu, Jie Wang, Jiecao Yu, Joanna Bitton, Joe Spisak, Jongsoo Park, Joseph Rocca, Joshua Johnstun, Joshua Saxe, Junteng Jia, Kalyan Vasuden Alwala, Kartikeya Upasani, Kate Plawiak, Ke Li, Kenneth Heafield, Kevin Stone, and et al. The llama 3 herd of models. arXiv preprint arXiv:2407.21783, 2024.
- [28] Jinze Bai, Shuai Bai, Shusheng Yang, Shijie Wang, Sinan Tan, Peng Wang, Junyang Lin, Chang Zhou, and Jingren Zhou. Qwen-VL: A versatile vision-language model for understanding, localization, text reading, and beyond. arXiv preprint arXiv:2308.12966, 2023.
- [29] Haoyu Lu, Wen Liu, Bo Zhang, Bingxuan Wang, Kai Dong, Bo Liu, Jingxiang Sun, Tongzheng Ren, Zhuoshu Li, Hao Yang, Yaofeng Sun, Chengqi Deng, Hanwei Xu, Zhenda Xie, and Chong Ruan. DeepSeek-VL: Towards real-world vision-language understanding. arXiv preprint arXiv:2403.05525, 2024.
- [30] Xiaokang Chen, Zhiyu Wu, Xingchao Liu, Zizheng Pan, Wen Liu, Zhenda Xie, Xingkai Yu, and Chong Ruan. Janus-Pro: Unified multimodal understanding and generation with data and model scaling. arXiv preprint arXiv:2501.17811, 2025.
- [31] Yash Goyal, Tejas Khot, Douglas Summers-Stay, Dhruv Batra, and Devi Parikh. Making the V in VQA matter: Elevating the role of image understanding in visual question answering. In *CVPR*, 2017.
- [32] Drew A. Hudson and Christopher D. Manning. GQA: A new dataset for real-world visual reasoning and compositional question answering. In CVPR, 2019.

- [33] Amanpreet Singh, Vivek Natarajan, Meet Shah, Yu Jiang, Xinlei Chen, Dhruv Batra, Devi Parikh, and Marcus Rohrbach. Towards VQA models that can read. In CVPR, 2019.
- [34] Bohao Li, Rui Wang, Guangzhi Wang, Yuying Ge, Yixiao Ge, and Ying Shan. SEED-Bench: Benchmarking multimodal LLMs with generative comprehension. *arXiv* preprint arXiv:2307.16125, 2023.
- [35] Yuan Liu, Haodong Duan, Yuanhan Zhang, Bo Li, Songyang Zhang, Wangbo Zhao, Yike Yuan, Jiaqi Wang, Conghui He, Ziwei Liu, Kai Chen, and Dahua Lin. MMBench: Is your multi-modal model an all-around player? In ECCV, 2024.
- [36] Weihao Yu, Zhengyuan Yang, Linjie Li, Jianfeng Wang, Kevin Lin, Zicheng Liu, Xinchao Wang, and Lijuan Wang. MM-Vet: Evaluating large multimodal models for integrated capabilities. In ICML, 2024.
- [37] Shuo Liu, Kaining Ying, Hao Zhang, Yue Yang, Yuqi Lin, Tianle Zhang, Chuanhao Li, Yu Qiao, Ping Luo, Wenqi Shao, and Kaipeng Zhang. ConvBench: A multi-turn conversation evaluation benchmark with hierarchical ablation capability for large vision-language models. In *NeurIPS*, 2024.
- [38] Ziyu Liu, Tao Chu, Yuhang Zang, Xilin Wei, Xiaoyi Dong, Pan Zhang, Zijian Liang, Yuanjun Xiong, Yu Qiao, Dahua Lin, and Jiaqi Wang. MMDU: A multi-turn multi-image dialog understanding benchmark and instruction-tuning dataset for LVLMs. In *NeurIPS*, 2024.
- [39] Holy Lovenia, Wenliang Dai, Samuel Cahyawijaya, Ziwei Ji, and Pascale Fung. Negative object presence evaluation (NOPE) to measure object hallucination in vision-language models. In *ACLW*, 2024.
- [40] Jiayu Wang, Yifei Ming, Zhenmei Shi, Vibhav Vineet, Xin Wang, Sharon Li, and Neel Joshi. Is a picture worth a thousand words? Delving into spatial reasoning for vision language models. In *NeurIPS*, 2024.
- [41] Jihan Yang, Shusheng Yang, Anjali W Gupta, Rilyn Han, Li Fei-Fei, and Saining Xie. Thinking in space: How multimodal large language models see, remember, and recall spaces. *arXiv preprint arXiv:2412.14171*, 2024.
- [42] Yinda Zhang, Shuran Song, Ping Tan, and Jianxiong Xiao. PanoContext: A whole-room 3D context model for panoramic scene understanding. In ECCV, 2014.
- [43] Hang Xu, Qiang Zhao, Yike Ma, Xiaodong Li, Peng Yuan, Bailan Feng, Chenggang Yan, and Feng Dai. PANDORA: A panoramic detection dataset for object with orientation. In *ECCV*, 2022.
- [44] Hao Chen, Yuqi Hou, Chenyuan Qu, Irene Testini, Xiaohan Hong, and Jianbo Jiao. 360+x: A panoptic multi-modal scene understanding dataset. In *CVPR*, 2024.
- [45] Qirui Wu, Sonia Raychaudhuri, Daniel Ritchie, Manolis Savva, and Angel X. Chang. R3DS: Reality-linked 3D scenes for panoramic scene understanding. In ECCV, 2024.
- [46] Yiyi Liao, Jun Xie, and Andreas Geiger. KITTI-360: A novel dataset and benchmarks for urban scene understanding in 2D and 3D. IEEE Transactions on Pattern Analysis and Machine Intelligence, 2023.
- [47] Chaoxiang Ma, Jiaming Zhang, Kailun Yang, Alina Roitberg, and Rainer Stiefelhagen. DensePASS: Dense panoramic semantic segmentation via unsupervised domain adaptation with attention-augmented context exchange. In *ITSC*, 2021.
- [48] Jieru Mei, Alex Zihao Zhu, Xinchen Yan, Hang Yan, Siyuan Qiao, Liang-Chieh Chen, and Henrik Kretzschmar. Waymo open dataset: Panoramic video panoptic segmentation. In *ECCV*, 2022.
- [49] Angel Chang, Angela Dai, Thomas Funkhouser, Maciej Halber, Matthias Niebner, Manolis Savva, Shuran Song, Andy Zeng, and Yinda Zhang. Matterport3D: Learning from RGB-D data in indoor environments. In 3DV, 2017.
- [50] Iro Armeni, Sasha Sax, Amir R. Zamir, and Silvio Savarese. Joint 2D-3D-semantic data for indoor scene understanding. arXiv preprint arXiv:1702.01105, 2017.
- [51] Heeseung Yun, Youngjae Yu, Wonsuk Yang, Kangil Lee, and Gunhee Kim. Pano-AVQA: Grounded audio-visual question answering on 360° videos. In ICCV, 2021.
- [52] Shih-Han Chou, Wei-Lun Chao, Wei-Sheng Lai, Min Sun, and Ming-Hsuan Yang. Visual question answering on 360° images. In WACV, 2020.
- [53] Chengshu Li, Fei Xia, Roberto Martín-Martín, Michael Lingelbach, Sanjana Srivastava, Bokui Shen, Kent Elliott Vainio, Cem Gokmen, Gokul Dharan, Tanish Jain, Andrey Kurenkov, C. Karen Liu, Hyowon Gweon, Jiajun Wu, Li Fei-Fei, and Silvio Savarese. iGibson 2.0: Object-centric simulation for robot learning of everyday household tasks. In *CoRL*, 2022.

- [54] Inpyo Song, Minjun Joo, Joonhyung Kwon, and Jangwon Lee. Video question answering for people with visual impairments using an egocentric 360-degree camera. In *CVPRW*, 2024.
- [55] Lianmin Zheng, Wei-Lin Chiang, Ying Sheng, Siyuan Zhuang, Zhanghao Wu, Yonghao Zhuang, Zi Lin, Zhuohan Li, Dacheng Li, Eric P. Xing, Hao Zhang, Joseph E. Gonzalez, and Ion Stoica. Judging LLM-as-a-judge with MT-bench and chatbot arena. In *NeurIPS*, 2023.
- [56] Machel Reid, Nikolay Savinov, Denis Teplyashin, Dmitry Lepikhin, Timothy P. Lillicrap, Jean-Baptiste Alayrac, Radu Soricut, Angeliki Lazaridou, Orhan Firat, Julian Schrittwieser, Ioannis Antonoglou, Rohan Anil, Sebastian Borgeaud, Andrew M. Dai, Katie Millican, Ethan Dyer, Mia Glaese, Thibault Sottiaux, Benjamin Lee, Fabio Viola, Malcolm Reynolds, Yuanzhong Xu, James Molloy, Jilin Chen, Michael Isard, Paul Barham, Tom Hennigan, Ross McIlroy, Melvin Johnson, Johan Schalkwyk, Eli Collins, Eliza Rutherford, Erica Moreira, Kareem Ayoub, Megha Goel, Clemens Meyer, Gregory Thornton, Zhen Yang, Henryk Michalewski, Zaheer Abbas, Nathan Schucher, Ankesh Anand, Richard Ives, James Keeling, Karel Lenc, Salem Haykal, Siamak Shakeri, Pranav Shyam, Aakanksha Chowdhery, Roman Ring, Stephen Spencer, Eren Sezener, et al. Gemini 1.5: Unlocking multimodal understanding across millions of tokens of context. arXiv preprint arXiv:2403.05530, 2024.
- [57] Josh Achiam, Steven Adler, Sandhini Agarwal, Lama Ahmad, Ilge Akkaya, Florencia Leoni Aleman, Diogo Almeida, Janko Altenschmidt, Sam Altman, Shyamal Anadkat, et al. GPT-4 technical report. arXiv preprint arXiv:2303.08774, 2023.

A Algorithm Detail

In this section, we provide more details on the construction pipeline for our OSR-Bench.

A.1 QA Pair Generation

Algorithm 2 details our systematic approach to generating question-answer pairs from omni-cognitive maps. For each scene, we generate three types of questions (object counting, relative distance, and relative direction) using structured templates. The algorithm takes as input an omni-cognitive map, a class count dictionary, and the expected max number of questions per type. We determine the expected maximum number of questions based on the similarity of the scenes to which the images correspond. For images obtained from DeepPanoContext [23], we set the expected number of questions to 10. For images obtained from ReplicaPano [22], we set the expected number of questions to 5.

To eliminate the duplication and ambiguity of the problem, we sample the objects in the scene without replacement and ensure the uniqueness of the positioning objects when generating non-negative sampling problems for relative distance and relative direction. In particular, if there are less than 5 object categories in the scene, we will not generate the above two types of problems. At the same time, we ensure that when generating relative direction problems, the three types of objects in the problem do not appear in the same cognitive map grid unit.

Algorithm 2 QA Pair Generation

```
Require: Omni-cognitve map C, Class count dictionary \mathcal{D}, Questions per type N
 1: Define Question Templates:
 2: T_{count} \leftarrow "How many object(s) are in this room?"
 3: T_{dist} \leftarrow "Measuring from the closest point of each object, which of these objects (candidates)
    is the closest to the positioning in this PANORAMA?
 4: T_{dir} \leftarrow "If I am standing by the positioning and facing the closest orienting, is the closest
    querying to my front, back, left, right, front-left, front-right, back-left, or back-right in this
    PANORAMA?"
 5: \mathcal{O} \leftarrow all object classes in \mathcal{D}
 6: \mathcal{O}_{unique} \leftarrow o \in \mathcal{O} \mid \mathcal{D}[o] = 1
 7: Q \leftarrow \emptyset
 8: // Generate object counting questions
 9: Sample \min(N, |\mathcal{O}|) objects from \mathcal{O} without replacement
10: for each sampled object o do
         q \leftarrow T_{count} with object replaced by o
11:
12:
         a \leftarrow \mathcal{D}[o] //answer for o
13:
         Add to Q
14: end for
15: // Generate relative distance questions
16: for i = 1 to N do
         Sample positioning object p from \mathcal{O}_{unique}
         Sample distinct candidates c_1, ..., c_4 from \mathcal{O} \setminus p
18:
         q \leftarrow T_{dist} with positioning replaced by p, candidates replaced by c_1, ..., c_4
19:
20:
         a \leftarrow c_i find by Euclidean distance in grid coordinates
21:
         Add to Q
22: end for
23: // Generate relative direction questions
24: for i = 1 to N do
         Sample positioning object p from \mathcal{O}_{unique}
25:
         Sample distinct orienting object o \in \mathcal{O} \setminus p and querying object q \in \mathcal{O} \setminus p, o
26:
27:
         q \leftarrow T_{dir} with positioning replaced by p, orienting replaced by o, and querying replaced
    by q
28:
         a \leftarrow Direction Computed based on vector relationships in grid coordinates
29:
         Add to Q
30: end for
31: return Q
```

A.2 Negative Sampling for Hallucination Testing

Algorithm 3 outlines our negative sampling strategy for evaluating model robustness against hallucination. We first compute global statistics on object frequency (as shown in Figure 6) and co-occurrence patterns across the dataset. For each scene, we identify two types of distractor objects: ① frequently occurring objects that are absent from the current scene (\mathcal{M}_f) and ② objects that commonly co-occur with present objects but are missing from the current scene (\mathcal{M}_c). These negative distractor objects are incorporated into the object pool used for Omni-Cognitive map generation prompt and QA generation. Specifically, we set the number of \mathcal{M}_f and \mathcal{M}_c for each image to 5 when performing negative sampling.

Algorithm 3 Negative Sampling for Hallucination Testing

```
Require: Omni-Cognitive map M, Parameters n, m
 1: Compute global object frequency statistics {\cal F} and global co-occurrence statistics {\cal C}
 2: Extract present objects \mathcal{P} from omni-cognitive map M
 3: \mathcal{M}_f \leftarrow \text{Top } n \text{ most frequent objects from } \mathcal{F} \text{ that are not in } \mathcal{P}
 4: \mathcal{M}_c \leftarrow \emptyset //Co-occurring but missing objects
 5: candidates \leftarrow \emptyset
 6: for each object p \in \mathcal{P} do
          for each object o co-occurring with p, sorted by co-occurrence frequency do
 7:
              if o \notin \mathcal{P} and o \notin \mathcal{M}_f and o \notin candidates then
 8:
                    candidates \leftarrow candidates \cup o
 9:
                    if |candidates| = m then
10:
11:
                        exit loop
12:
                    end if
13:
              end if
14:
          end for
15: end for
16: \mathcal{M}_c \leftarrow \text{Top } m \text{ objects from } candidates
17: \mathcal{O}_{aug} \leftarrow \mathcal{P} \cup \mathcal{M}_f \cup \mathcal{M}_c //Augmented object set
18: Generate QA pairs using \mathcal{O}_{aug} with rules:
        - For counting: Return 0 for objects in \mathcal{M}_f \cup \mathcal{M}_c
        - For spatial questions: Return appropriate "not found" responses when needed
21: return QA pairs with both real and hallucinated objects
```

B Dataset Detail

This section provides statistical insights into the composition and characteristics of our OSR-Bench dataset.

Our dataset contains a large number of question-answer pairs across different reasoning categories. For the standard dataset, we have a total of 74, 326 questions distributed as follows:

```
Relative distance questions: 26, 240
Object counting questions: 24, 988
Relative direction questions: 23, 098
```

For the dataset with negative sampling , we have 78, 986 questions distributed as:

```
Object counting questions: 27, 125
Relative distance questions: 26, 250
Relative direction questions: 25, 611
```

Figures 7-9 present the answer distributions for each question type, both with and without negative sampling.

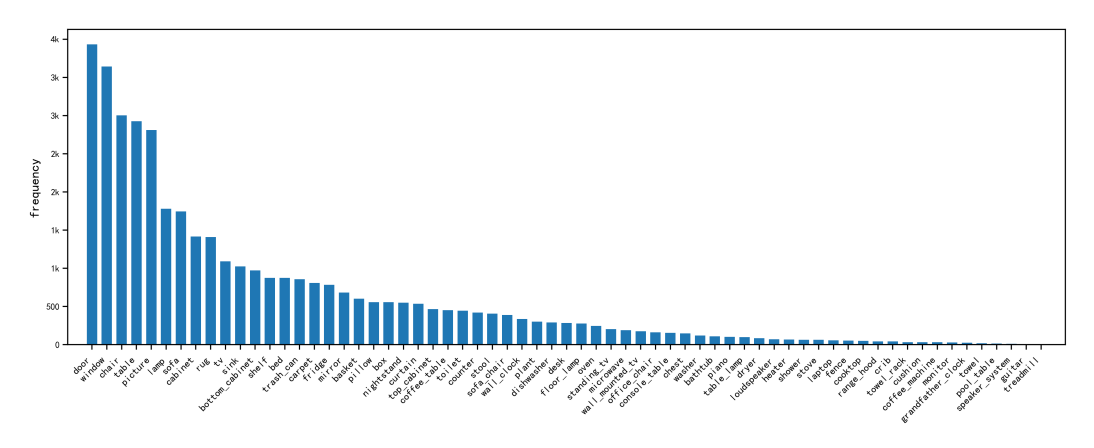


Figure 6: Object frequency of the entire dataset.

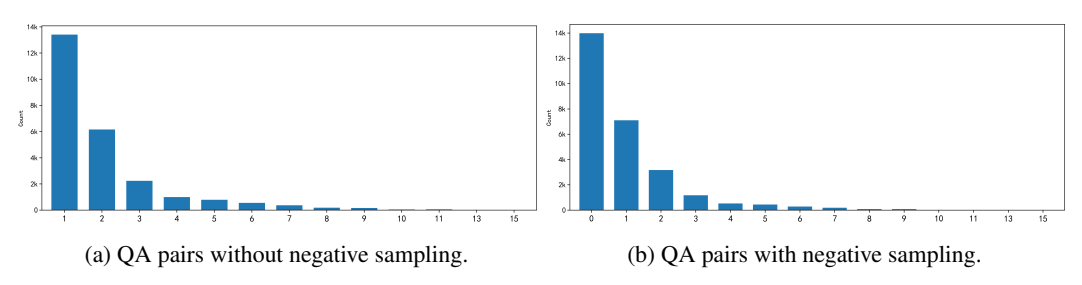


Figure 7: Answer distribution of Object Counting question.

C Prompt Template

This section details the prompt templates used throughout our evaluation pipeline.

C.1 Omni-Cognitive Map Generate Prompt

The cognitive map generation prompt instructs models to analyze a panoramic image and construct a structured spatial representation of the scene. In actual application, in the case of non-negative sampling, we fill the {object_pool} with the object categories contained in the Ground truth. In the case of negative sampling, we add negative distractor objects to the {object_pool}.

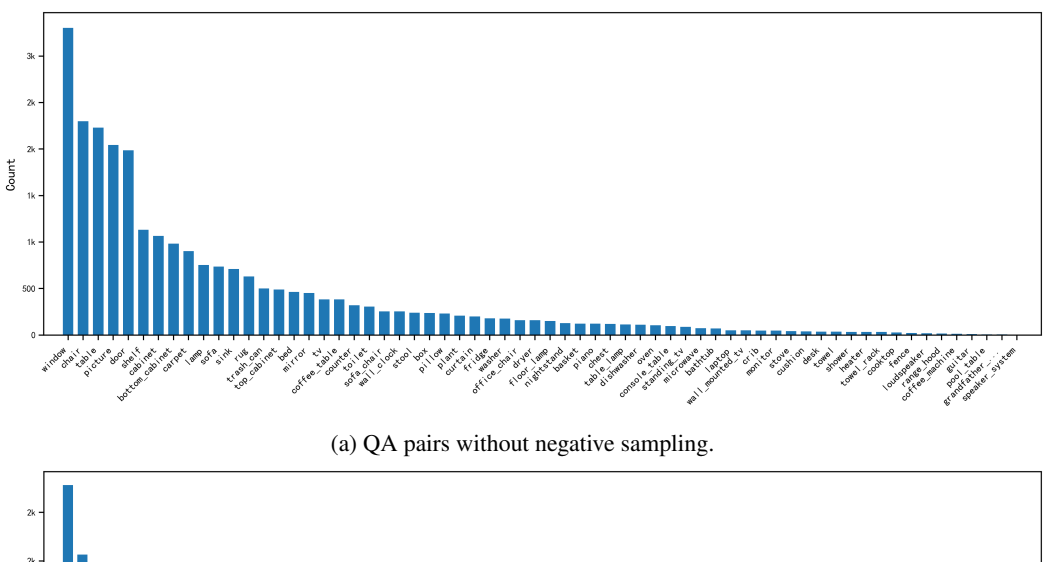
Cognitive Map Prompt

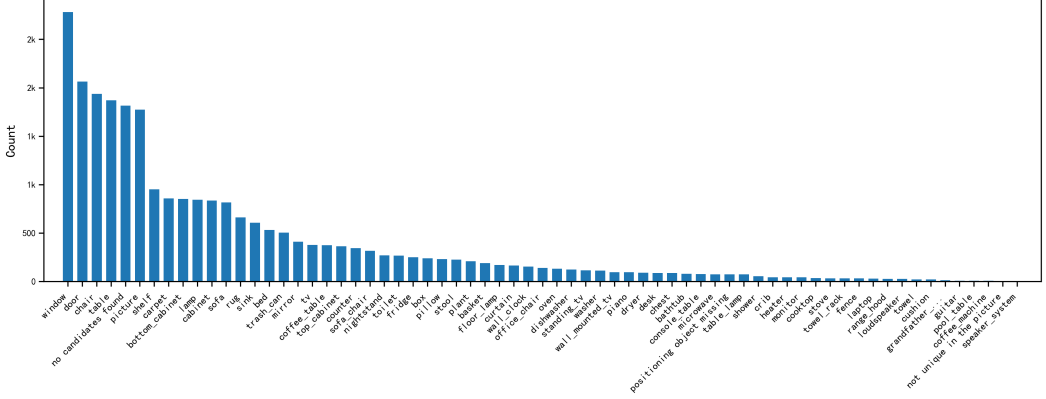
[Task]

This PANORAMA captures an indoor scene. Your objective is to identify specific objects within the panorama, understand the spatial arrangement of the scene, and estimate the center point of each object, assuming the entire scene is represented by a 10x10 grid.

[Rule]

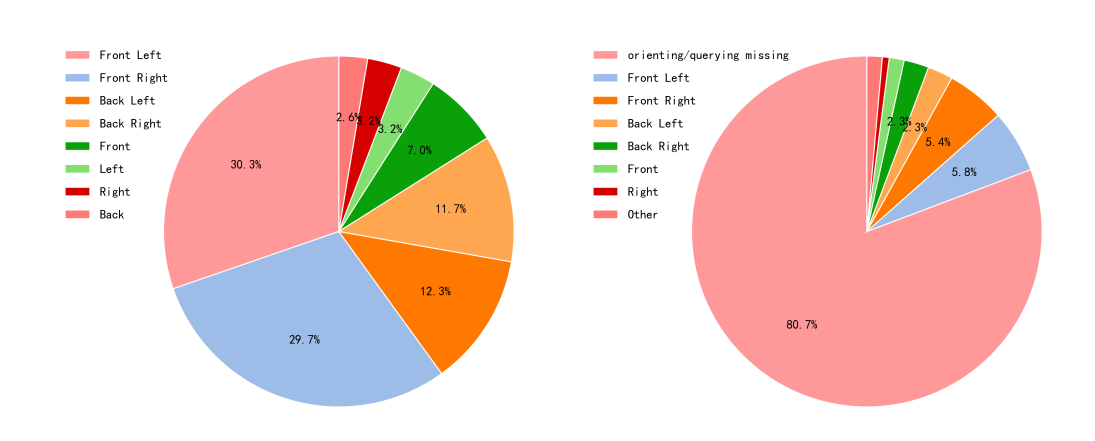
- 1. We provide the categories to care about in this scene: {object_pool} . Focus ONLY on these categories.
- 2. Estimate the center location of each instance within the provided categories, assuming the entire scene is represented by a 10x10 grid.
- 3. If a category contains multiple instances, include all of them.
- 4. Each object's estimated location should accurately reflect its real position in the scene, preserving the relative spatial relationships among all objects.
- 5. Consider object distance from camera when positioning them. Closer objects should be placed near the center of the grid, while distant objects should be placed toward the edges.
- 6. If an object is partially visible or occluded, estimate its full position based on the visible parts.





(b) QA pairs with negative sampling.

Figure 8: Answer distribution of Relative Distance question.



(a) QA pairs without negative sampling.

(b) QA pairs with negative sampling.

Figure 9: Answer distribution of Relative Direction question.

[Output]

Present the estimated center locations for each object as a list within a dictionary. STRICTLY follow this JSON format And use INTEGERS within 10 to represent the coordinates: {"category name": $[(x_1, y_1), ...], ...$ }

C.2 Pre and Post Prompt

When we do not prompt the model to generate cognitive maps but ask it to answer questions directly, we add a pre-prompt before the question. The input for the models is formatted as follows: [Image Token] [Pre-prompt] [Question] [Post-prompt]

Figure 10 shows our complete reasoning process, which includes two evaluation modes: "Vanilla Mode" and "Think Mode". We switch between the two modes by using different post-prompts.

Pre-Prompt

According to the PANORAMA and the predicted objects' center locations, answer the following question:

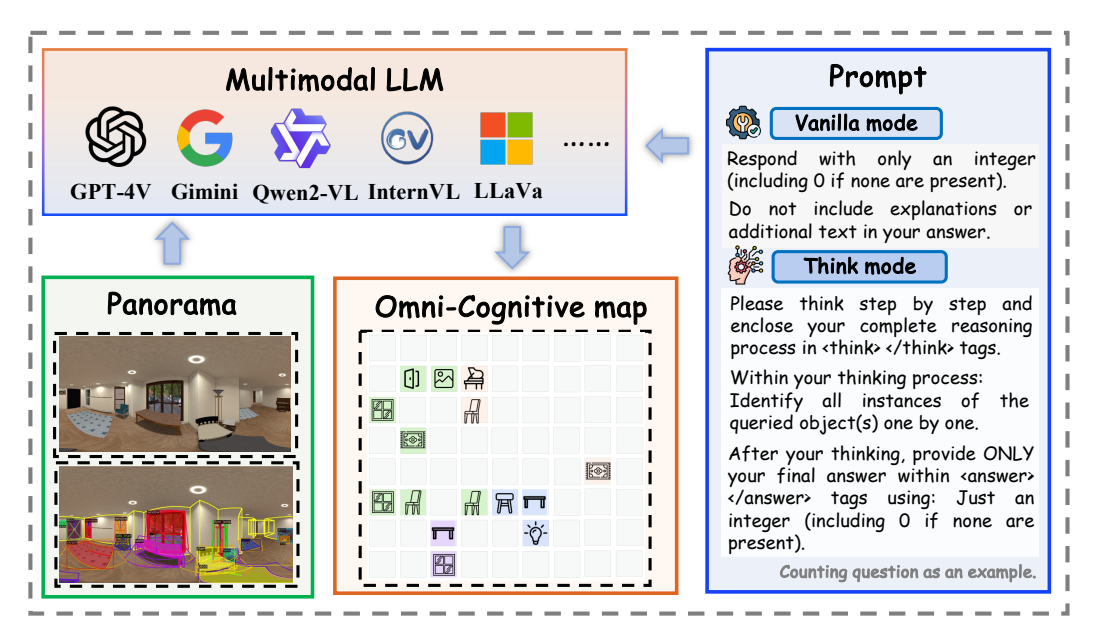


Figure 10: Inference pipeline.

C.3 LLM Evaluator Prompt

The LLM evaluator prompts enable automatic assessment of model responses, particularly for complex cases where rule-based evaluation may be insufficient. We provide three distinct evaluator prompts for the different question types. Each prompt includes specific evaluation rules and a structured JSON response format with both a binary score and confidence level. This approach ensures consistent assessment across diverse response formats from different models, especially for cases involving negative sampling where proper handling of non-existent objects is crucial. Specifically, we use DeepSeek-V3 as the evaluator, and replace {question}, {ground_truth}, {model_answer} in the template with the real case.

```
You are evaluating an object counting answer.

Question: {question}

Ground Truth: {ground_truth}

Model Answer: {model_answer}

Evaluation rules:

- The answer must be an integer (including 0)

- Correct if the model's integer exactly matches the ground truth

- Also correct if the model answer contains additional text but has the correct number Please respond in JSON format:

{
    "score": 0 or 1,
    "confidence": "high" or "middle" or "low"
}
```

META_PROMPT_RELATIVE_DISTANCE

```
You are evaluating a relative distance answer.
```

Question: {question}

Ground Truth: {ground_truth}

Model Answer: {model answer}

Evaluation rules:

- Normal answers are object names
- Special case answers may be one of these error messages:
- "The positioning object is not found in the picture."
- "The positioning object is not unique in the picture."
- "None of the candidates were found in the picture."
- When the ground truth is one of these special error messages, the model answer must match exactly
- When the ground truth is an object name, the model answer is correct if it contains the matching object name (case insensitive)

Please respond in JSON format:

```
{
"score": 0 or 1,
"confidence": "high" or "middle" or "low"
}
```

META_PROMPT_RELATIVE_DIRECTION

You are evaluating a relative direction answer.

Question: {question}

Ground Truth: {ground_truth}

Model Answer: {model_answer}

Evaluation rules:

- Normal answers are direction words: "Front", "Back", "Left", "Right", "Front-Left", "Front-Right", "Back-Left", "Back-Right"
- Direction words are case insensitive, and hyphens are optional (e.g., "front left" equals "Front-Left")
- Special case answers may be one of these error messages:
- "The positioning object is not found in the picture."
- "The positioning object is not unique in the picture."
- "The orienting object or querying object is not found in the picture."

```
- When the ground truth is one of these special error messages, the model answer must match exactly
Please respond in JSON format:
{
"score": 0 or 1,
"confidence": "high" or "middle" or "low"
}
```

D Evaluation Details

To ensure reproducibility, we adopt a greedy decoding strategy for all models (*i.e.*, the temperature is set to 0, and both top-p and top-k are set to 1 for proprietary models, do_sample is set to False for open-source models).

A complete evaluation task (*i.e.*, evaluating a specific model with or without a omni-cognitive map, in vanilla or think mode, on a non-negative or negative sampling dataset) requires approximately 4-5 days. For hardware requirements, models below 13B parameters use 1 NVIDIA A40 48G GPU, models between 13B and 30B use 3 NVIDIA A40 48G GPUs, while models exceeding 70B parameters require 3 NVIDIA A800 80G GPUs.

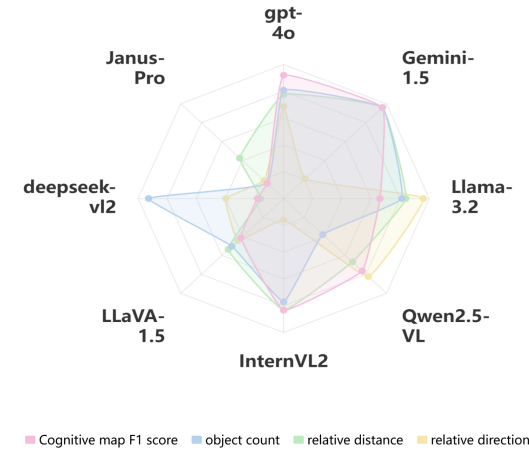


Figure 11: *OSR*-benchmark Overview

E More Cases

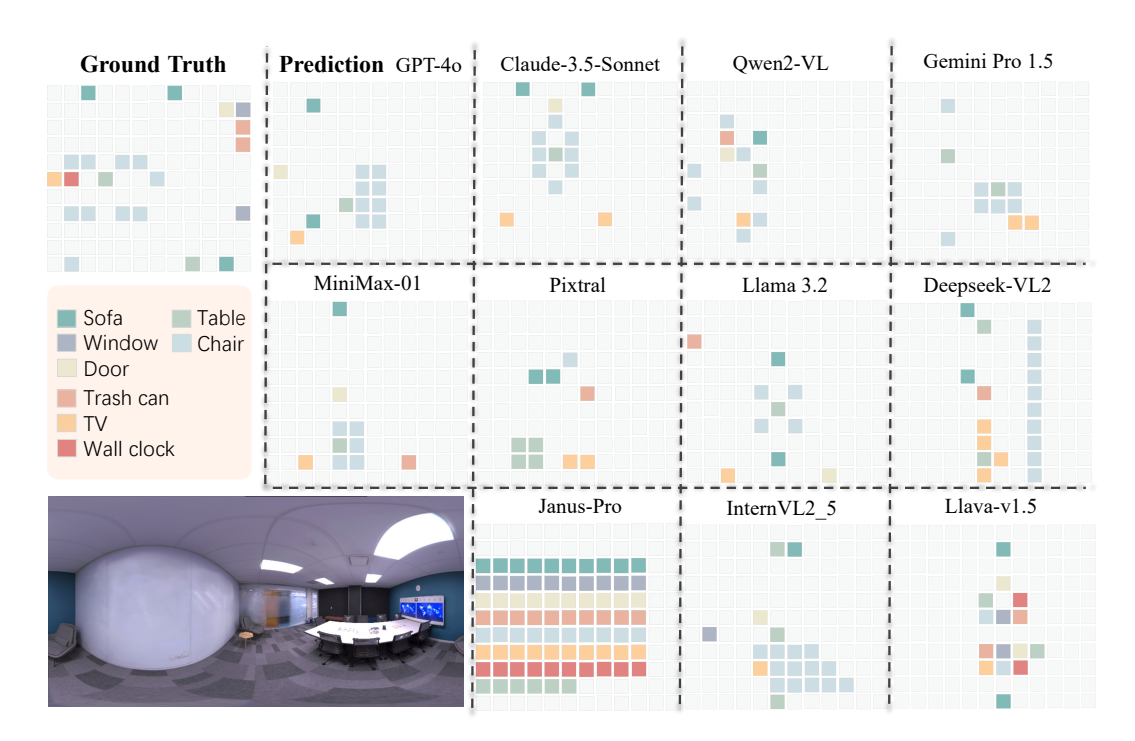


Figure 12: Visualization of Omni-Cognitive map generation



Figure 13: Good case in think mode